Journal of the Serbian Chemical Society
JSCS-info@shd.org.rs • www.shd.org.rs/JSCS
J. Serb. Chem. Soc. *83* (1) 1–18 (2018)
JSCS–5054
UDC 547.572.3–304.2+547.261'451.64:
544.431.143:541.124.7+519.677
Original scientific paper

4-[(4-Acetylphenyl)amino]-2-methylidene-4-oxobutanoic acid, a newly synthesized amide with hydrophilic and hydrophobic segments: Spectroscopic characterization and investigation of its reactive properties

SHEENA Y. MARY[1], EBTEHAL S. AL-ABDULLAH[2], HAYA I. ALJOHAR[2], BADIADKA NARAYANA[3], PRAKASH S. NAYAK[3], BALADKA K. SAROJINI[4], STEVAN ARMAKOVIĆ[5], SANJA J. ARMAKOVIĆ[6#], CHRISTIAN VAN ALSENOY[7] and ALI A. EL-EMAM[2]*

[1]Department of Physics, Fatima Mata National College, Kollam, Kerala, India, [2]Department of Pharmaceutical Chemistry, College of Pharmacy, King Saud University, Riyadh 11451, Saudi Arabia, [3]Department of Studies in Chemistry, Mangalore University, Mangalagangothri, Mangalore 574199, India, [4]Department of Studies in Industrial Chemistry, Mangalore University, Mangalagangothri, Mangalore 574199, India, [5]University of Novi Sad, Faculty of Sciences, Department of Physics, Trg D. Obradovića 4, 21000 Novi Sad, Serbia, [6]University of Novi Sad, Faculty of Sciences, Department of Chemistry, Biochemistry and Environmental Protection, Trg D. Obradovića 3, 21000 Novi Sad, Serbia and [7]Department of Chemistry, University of Antwerp, Groenenborgerlaan 171, B-2020, Antwerp, Belgium

(Received 3 January, revised 17 March, accepted 16 May 2017)

Abstract: The FT-IR and FT-Raman spectra of 4-[(4-acetylphenyl)amino]-2--methylidene-4-oxobutanoic acid were recorded. The vibrational wave numbers were computed by DFT quantum chemical calculations and the vibrational assignments were realized using the potential energy distribution. The theoretically predicted geometrical parameters were in agreement with the XRD data. Determination and visualization of molecule sites prone to electrophilic attacks were performed by mapping the average local ionization energies (*ALIE*) to the electron density surface. Furthermore, determination of possible reactive centres of title molecule was realized by calculation of the Fukui functions. Intramolecular non-covalent interactions were also determined and visualized. In addition, prediction of molecule sites possibly prone to autoxidation was performed by calculation of the bond dissociation energies (*BDE*), while the stability of the title molecule in water was assessed by calculation of radial distribution functions (RDF) obtained after molecular dynamics (MD) simulations.

* Corresponding author. E-mail: elemam5@hotmail.com
# Serbian Chemical Society member.
https://doi.org/10.2298/JSC170103056M

The docked title ligand compound forms a stable complex with insulin receptor kinase and gives a binding affinity of –10.2 kcal* mol^{-1}.

Keywords: DFT; ALIE; BDE; RDF; molecular docking.

INTRODUCTION

Copolymers containing both hydrophilic and hydrophobic segments are drawing considerable attention because of their possible use in biological systems. *N*-Substituted itaconamic acids are strongly amphiphilic molecules.[1] Itaconic anhydride is an unsaturated organic dicarbonic anhydride with one carbonyl group conjugated to the methylene group and can be regarded as a substituted acrylic or methacrylic derivative and it can be obtained from renewable resources.[2] Itaconic anhydride derivatives are useful for the synthesis of various biodynamic derivatives such as imides, oxazepine and oxobutanoic acid.[3–6] Amide bonds, which play major roles in the elaboration and composition of biological systems, are the main bonds that link amino acid building blocks together to give proteins and these types of bonds are not limited to biological systems and are indeed present in a huge array of molecules including major marketed drugs. Amide derivatives were reported to possess anti-inflammatory,[7–9] antitubercular,[10,11] and anti-proliferative[12] activities.

Due to highly frequent use and improper disposal, pharmaceutical molecules significantly accumulate in all types of waters and exhibit harmful effects towards aquatic organisms.[13,14] Additionally, these molecules are synthesized to be very stable and thus their removal is very difficult under natural conditions, while simultaneously, conventional procedures for their removal from water are not efficient.[15,16] For the removal of pharmaceutical molecules from water, scientists have developed forced degradation procedures based on advanced oxidation processes.[14,15,17–21] These efforts are tedious and time consuming and there is constant need for rationalization and optimization of these procedures. In this regard, DFT calculations and molecular dynamics (MD) simulations have been readily employed,[22–25] since they are valuable for the prediction of the reactive properties of investigated molecules by relatively inexpensive computational experiments. Information on local reactivity properties obtained by molecular modelling principles is also valuable for the determination and validation of degradation mechanisms.[15] In this work, a complete vibrational spectroscopic analysis of 4-[(4-acetylphenyl)-amino]-2-methylidene-4-oxobutanoic acid was performed by combining experimental and quantum chemical calculations, including molecular dynamics simulations.

EXPERIMENTAL

The title compound ($C_{13}H_{13}NO_4$) was prepared in 87 % yield *via* the reaction of 3-methylidenedihydrofuran-2,5-dione with 4′-aminoacetophenone at room temperature as previously described.[26]

* 1 kcal = 4184 J

The FT-IR spectrum of the title compound was recorded using KBr pellets on a DR/ /Jasco FT-IR spectrometer. The FT-Raman spectrum was obtained on a Bruker RFS 100/s instrument.

Quantum chemical calculations

The quantum chemical calculations of the title compound were performed with the Gaussian'09 program,[27] using the B3LYP/6-311++G(d) (5D, 7F) basis set to predict the molecular structure and frequencies. A scaling factor of 0.9613 had to be used to obtain a considerably better agreement with the experimental data.[28] The structural parameters with XRD data corresponding to the optimized geometry of the title compound (Fig. 1) are given in Table S-I of the Supplementary material to this paper. The assignments of the calculated frequencies were realized using Gaussview[29] and GAR2PED[30] software.

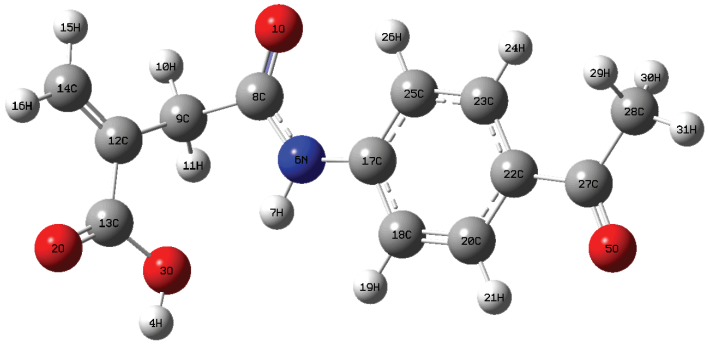

Fig. 1. Optimized geometry of 4-[(4-acetylphenyl)amino]-2-methylidene-4-oxobutanoic acid.

The Jaguar 9.0 program[31] was used for the DFT calculations and the Desmond program[32-34] was used for the MD simulations, both as implemented in the Schrödinger Materials Science Suite 2015-4. The B3LYP exchange-correlation functional[35] was used for the DFT calculations by the Jaguar program, with 6-311++G(d,p), 6-31+G(d,p) and 6-311G(d,p) basis sets for the calculations of the average local ionization energies (*ALIE*), Fukui functions and bond dissociation energies (*BDEs*), respectively. The MD simulations were conducted by the OPLS 2005 force field[36] with the simulation time set to 10 ns and with the isothermal–isobaric (NPT) ensemble class. The MD system was modelled by placing one title molecule into a cubic box with ≈2500 water molecules. The temperature was 300 K, the pressure 1.0325 bar and the cut-off radius was 12 Å. Concerning the solvent, a simple point charge (SPC) model was used.[37] Non-covalent interactions were investigated by the method of Johnson *et al.*[38,39] When the Schrödinger Materials Science Suite 2015-4 was used, Maestro GUI[40] was used for the preparation of input files and analysis of the results. Charge transfer within the molecule was investigated by the Multiwfn program for the analysis of wave function.[41-44]

RESULTS AND DISCUSSION

Geometrical parameters

The values of the C–N bond lengths (DFT/XRD) C_{17}–N_6 = 1.4056/1.4202 Å, C_8–N_6 = 1.3756/1.3542 Å indicated that the C–N bonds showed partial double bond character in this fragment and were found to be much more shorter

than the average value for a single C–N bond (1.47 Å), but significantly longer than a C=N double bond (1.22 Å), suggesting some multiple bond character is present.[45] The C=O bond lengths (DFT/XRD) in the present case were 1.2043/ /1.2492, 1.2164/1.2222, 1.2186/1.2162 Å and C–O bond length (DFT/XRD) was 1.3720/1.2882 Å, which are in agreement with the reported values.[46,47] The C=C bond length (DFT/XRD) was 1.3369/1.3282 Å and the C–C bond lengths (DFT/XRD) were in the range 1.4922–1.5388/1.4852–1.5232 Å, which are in agreement with the reported values.[45,47] The C–C bond lengths (DFT/XRD) in the phenyl ring lie between 1.3822–1.4068/1.3802–1.3972 Å. For the title compound, the benzene ring is a regular hexagon with bond lengths somewhere in between the normal values for a single and double bond (1.54 Å and 1.33 Å).[45,48] At the C_{22} position, the bond angles (DFT/XRD) are C_{23}–C_{22}–C_{20} = 118.1/ /118.1, C_{23}–C_{22}–C_{27} = 123.2/123.1° and C_{20}–C_{22}–C_{27} = 118.7/118.2°, with this asymmetry showing interaction between C_{27}–O_5 with the H_{21} atom. Similarly, at the C_{17} position, the bond angle C_{18}–C_{17}–C_{25} is reduced by 0.8°, C_{18}–C_{17}–N_6 is reduced by 2.9° and C_{25}–C_{17}–N_6 is increased by 3.7° and at the N_6 position, the angle C_{17}–N_6–C_8 is increased by 9.0°, C_{17}–N_6–H_7 is reduced by 4.4° and C_8–N_6–H_7 is reduced by 4.7° from 120°, which shows the interaction between the phenyl ring and the CONH group. The interaction of CH_2 at C_9 and C_8–O_1 were revealed from the bond angles N_6–C_8–O_1 = 124.7°, N_6–C_8–C_9 = 114.1° and O_1–C_8–C_9 = 121.2°. The asymmetry of the bond angles at the C_{13} position (O_2–C_{13}–O_3 = 121.1°, O_2–C_{13}–C_{12} = 126.5° and O_3–C_{13}–C_{12} = 112.3°) shows the interaction between the CH_2 group at C_9 and the carboxylic group.

IR and Raman spectra

The vibrational spectral analysis was performed based on the characteristic vibrations of the amide (CONH), carboxyl (COOH), acetyl ($COCH_3$), C=C, C–C, methylene (CH_2) and phenyl ring modes. The computed vibrational wave numbers, IR, Raman intensities, measured IR and Raman band positions and their assignments are given in Table S-2 of the Supplementary material. The simulated and observed FT-IR and Raman spectra are shown in Figs. S-1 and S-2 of the Supplementary material, respectively.

Amide (CONH) vibrations. The C=O stretching and deformation modes were assigned at 1665 (IR), 1661 (Raman), 1672 (DFT) and 798, 613 (IR), 798, 615 (Raman), 801 and 613 cm^{-1} (DFT), which are in agreement with the reported literature.[49–51] The C=O stretching mode is active in both the IR and Raman spectra with high IR intensity and Raman activity with a PED (potential energy distribution) of 78 %, which is a pure mode. The PED of the deformation modes are 40 and 37 % and the Raman activities are low with moderate IR intensities. Raju *et al.* reported the C=O modes at 1654, 795, 580 (IR), 1659, 798 and 577 cm^{-1} (DFT), for a related derivative.[45] The N–H stretching mode is expected in

the region 3500–3300 cm^{-1} and the N–H deformation at around 1500 cm^{-1} and 125 cm^{-1}.[50,52] For the title compound, these modes were assigned at 3297 (IR), 3434 (DFT) (stretching), 1240 (IR), 1483, 1238 cm^{-1} (DFT). In the present case, the NH stretching mode is downshifted from the computed value by 137 cm^{-1}, which indicates hydrogen bonding in the system and has high IR intensity. The PEDs of the NH deformation modes were around 48 % and the IR intensity of the mode 1483 cm^{-1} is very low and no bands were seen in the IR spectrum while the mode at 1238 cm^{-1} has high IR intensity and a corresponding band is observed in the IR spectrum at 1240 cm^{-1}. The N–H modes were reported at 3281 (IR), 3405 (DFT) (stretching), 1541, 1256 (IR), 1551, 1255 (DFT),[45] and 1587, 1250, 650 (IR), 1580, 1227 and 652 cm^{-1} (DFT).[53] In the present case, the N–H out-of-plane mode was assigned at 670 cm^{-1} in the IR, 664 cm^{-1} in the Raman spectrum and at 661 cm^{-1} theoretically.[49] The reported values for similar derivatives were 762 (IR), 757 (DFT),[41] and 650 (IR), 652 cm^{-1} (DFT).[53] The C–N stretching modes were assigned at 1225 (IR) and 1234, 1231 cm^{-1} (DFT) for the title compound, which are in agreement with the literature.[45]

Carboxyl (COOH) modes. For the title compound, the COOH modes are assigned at 3564 cm^{-1} (IR), 3585 cm^{-1} (DFT, OH stretching mode), 1695 cm^{-1} (IR), 1694 cm^{-1} (DFT, C=O stretching mode), 517 cm^{-1} (IR), 685, 519 cm^{-1} (DFT, C=O deformation modes), 1308 cm^{-1} (Raman), 1308, 965 cm^{-1} (DFT, OH in-plane and out-of-plane deformation) and 1234 cm^{-1} (DFT, C–O stretching) as expected in literature.[49,50] The carbonyl stretching mode at 1694 cm^{-1} possesses a high IR intensity and has a PED of 72 % and the deformation modes have PEDs around 40 %. The OH in-plane and C–O stretching modes have high IR intensities. The reported values are 1680, 561 (IR), 1675, 735, 555 (DFT) for the C=O group, 1321 (IR), 1318, 920 (DFT) for the OH group and 1235 (IR), 1238 cm^{-1} (DFT) for C–O, for a similar derivative.[45]

Acetyl ($COCH_3$) modes. Aromatic acetyl groups exhibit methyl stretching modes in the region 3040–2900 cm^{-1}.[49] The methyl stretching modes were assigned at 3025, 2972 and 2928 in the IR spectrum, 2970 and 2930 in the Raman spectrum, and at 3024, 2974 and 2920 cm^{-1} theoretically. The methyl deformation modes were assigned at 1433 and 1345 in the IR spectrum, 1438 and 1355 in the Raman spectrum, and at 1440, 1431 and 1346 cm^{-1} theoretically, which are expected in the region 1480–1340 cm^{-1}.[49] The methyl rocking modes are expected in the range 1080–900 cm^{-1},[49] and in the present case, these modes were assigned at 1050 and 1013 in IR, 1008 in Raman and at 1052 and 1011 cm^{-1} theoretically.

C=C, C–C and CH_2 modes. For the title compound, C=C and C–C stretching modes were assigned at 1610 cm^{-1} (IR) and 1600 cm^{-1} (Raman), 1617 cm^{-1} (DFT, C=C) and 1090, 927 and 739 cm^{-1} (IR), 1084, 921 and 739 cm^{-1} (Raman), 1082, 940, 924 and 739 cm^{-1} (DFT) as expected.[49–51] In the present

case, the CH_2 modes were assigned at 3008 and 2954 cm^{-1} (IR), 3009 and 2950 cm^{-1} (Raman), 3121, 3033, 3012 and 2956 cm^{-1} (DFT, stretching modes), 1384, 1273, 1240 and 1112 cm^{-1} (IR), 1438, 1381, 1272 and 1115 cm^{-1} (Raman) and in the range 1440–911 cm^{-1} (DFT, deformation modes).[49–51,54]

Phenyl ring modes. The C–H stretching modes of the phenyl ring are expected above 3000 cm^{-1}.[49] In the present case, the bands observed at 3075 and 3064 in the IR spectrum, 3079, 3062 and 3030 in the Raman spectrum and 3122, 3078, 3066 and 3031 cm^{-1} theoretically were assigned as these modes. The phenyl ring C–C stretching modes are observed at 1590, 1580, 1505 and 1302 in the IR spectrum and 1506 cm^{-1} in the Raman spectrum. The corresponding theoretical values were 1586, 1574, 1508, 1389 and 1300 cm^{-1} with PEDs in between 41 to 60 %. The ring breathing mode was observed at 836 cm^{-1} in the IR spectrum, which finds support from the computational value at 835 cm^{-1} as expected with a PED of 43 %.[49,55] The C–H deformation modes of the phenyl ring are expected above 1000 cm^{-1} (C–H in-plane bending) and below 1000 cm^{-1} (CH out-of-plane bending).[49] For the title compound, these deformation bands were assigned at 1285, 1157 and 988 cm^{-1} (IR), 1162 cm^{-1} (Raman), 1288, 1159, 1105 and 990 cm^{-1} (DFT, in-plane bending) and 945 and 810 cm^{-1} (IR), 946 and 824 cm^{-1} (Raman), and 943, 941, 826 and 807 cm^{-1} (DFT, out-of-plane bending).

Frontier molecular orbitals

The frontier molecular orbitals and their properties, such as energy, are very useful for predicting the most reactive position in a π-electron system and several types of reactions in conjugated systems.[56] The energy of the highest occupied molecular orbital (HOMO) is directly related to the ionization potential and characterizes the susceptibility of the molecule towards the attack of electrophiles and the energy of the lowest unoccupied molecular orbital (LUMO) is related to the electron affinity and characterizes the susceptibility of the molecule towards attack by nucleophiles.[57] The HOMO and LUMO energy values for the investigated compound are –6.656 and –2.324 eV and the energy gap is 4.332 eV, which clearly indicates that charge transfer occur within the molecule, which increases the molecular activity. The HOMO and LUMO molecular orbitals are shown in Fig. 2. The various chemical descriptors are: hardness $\eta = (I–A)/2 =$ 2.166 eV, chemical potential $\mu = –(I+A)/2 = –4.49$ eV and global electrophilicity index $\omega = \mu^2/2\eta = 4.654$ eV, where $I = –E_{HOMO} = 6.656$ eV and $A = –E_{LUMO} = 2.324$ eV are the first ionization potential and electron affinity, respectively.[58]

Understanding of the charge transfer within a molecule is of great importance.[59] In order to confirm the charge transfer within the molecule, an analysis of the charge transfer for electron excitation based on the electron density difference was also performed. The analysis of the charge transfer between the first singlet

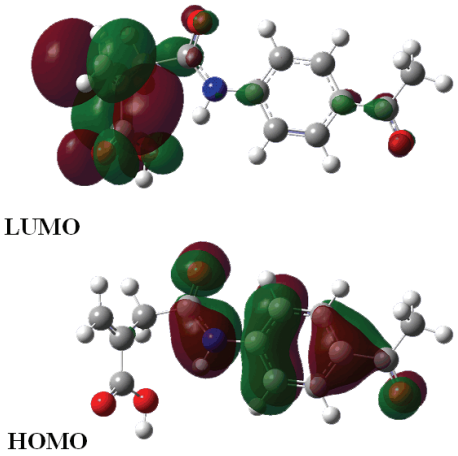

Fig. 2. HOMO–LUMO structures of 4--[(4-acetylphenyl)amino]-2-methylidene-4--oxobutanoic acid.

excited and ground states of the title compound was performed according to a reported method,[60] as implemented in the Multiwfn program. It should be noticed that the described method[60] provided for the case of charge transfer in one dimension, while in the case of the implementation in the Multiwfn program, the method was generalized in three dimensions. According to the previous study,[60] the charge transfer can be quantified by the charge transfer (CT) length. The CT length is defined as a distance between barycentres of C_+ and C_- functions, which are defined on the basis of the electron density variation between the excited and ground states. In this work, the CT length was calculated employing the Multiwfn program. The barycentres of the positive and negative parts of C_+ and C_- are visualized in Fig. 3, together with the calculated CT length. According to the results provided in Fig. 3, it could be concluded that the CT length has value of 3.16 Å. This high value of the CT length clearly indicates the charge transfer nature of excitation, while the positions of the C_+ and C_- functions indicate that charge transfer occurs from the part of molecule containing C8–O1 to the phenyl group. The fact that the aforementioned charge transfer occurs is also complemented by the calculation of Δr coefficient according to the literature.[61] The lower the Δr parameter is, the more likely is that the excitation is of a local type (LE). However, in the present case, the Δr has a high value of 4.17 Å, which clearly confirms the CT nature of the excitation. The Mutliwfn program was also employed for the calculation of Δr index.

Molecular electrostatic potential

The molecular electrostatic potential (MEP) is related to the electronic density and is a very useful descriptor for determining the sites for electrophilic and nucleophilic reactions.[62] The different values of the electrostatic potential are represented by different colours and the potential increases in the order red <

< orange < yellow < green < blue. In the MEP, the maximum negative region represents the site for electrophilic attack, indicated by the red colour, while the maximum positive region represents nucleophilic attack, indicated by the blue colour. As seen from the MEP map of the investigated compound (Fig. 4), the regions of negative potential are over the electronegative oxygen atoms of the carbonyl groups and the regions having the positive potential are over the hydrogen atoms.

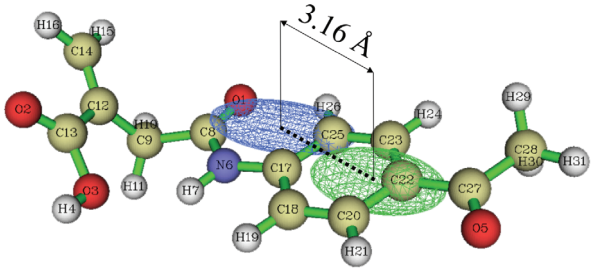

Fig. 3. C_+ (green) and C_- (blue) functions and visualization of their barycentres.

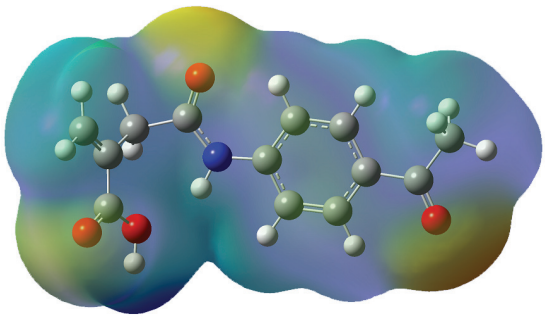

Fig. 4. MEP plot of 4-[(4-acetylphenyl)amino]-2-methylidene-4-oxobutanoic acid.

ALIE surface, Fukui functions and non-covalent interactions

To obtain a clearer picture on the local reactivity properties of the title molecule, reference will be made to the average local ionization energy (*ALIE*), which is a quantity that provides information on the energy required for the removal of electron from some point in space around the molecule. The lowest values of this quantity practically indicate the molecule sites where electrons are least tightly bonded to the molecule and, therefore, are the molecule sites that are prone to electrophilic attacks. *ALIE* was introduced by Politzer *et al.*,[63,64] and it is defined as sum of orbital energies weighted by the orbital densities according to the following equation:

$$I(r) = \sum_i \frac{\rho_i(\vec{r})|\varepsilon_i|}{\rho(\vec{r})} \quad (1)$$

where $\rho_i(\vec{r})$ denotes the electronic density of the *i*-th molecular orbital at the point $\vec{r}$, ε_i denotes orbital energy, while $\rho(\vec{r})$ denotes the total electronic density function.[65,66] In this work, the *ALIE* values were mapped to the electron density (Fig. 5).

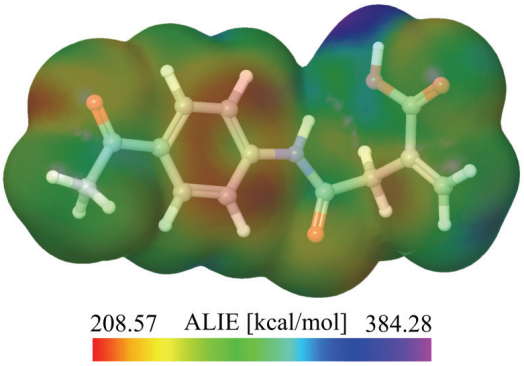

Fig. 5. *ALIE* surface of 4-[(4-acetylphenyl)amino]-2-methylidene-4-oxobutanoic acid.

The *ALIE* surface of the investigated molecule indicates that there are three specific locations possibly prone to electrophilic attacks. These molecule sites are the benzene ring, near vicinity of the oxygen atom O5 and near vicinity of the carbon atom C9. These locations are characterized by the lowest *ALIE* values (red colour in Fig. 5) of ≈209 kcal mol^{-1}. On the other hand, the highest *ALIE* values were calculated to be in the near vicinity of hydrogen atom H4, characterized by a value of 384 kcal mol^{-1} (blue colour in Fig. 5). The distribution of the *ALIE* values indicates relatively high reactivity of the molecule. The molecule is also characterized by the formation of two intramolecular non-covalent bonds located between the O3–H7 atoms and the O1–H26 atoms. Both of the aforementioned non-covalent interactions have practically the same values of strength, expressed in terms of electron/bohr^3* (Fig. 6).

The local reactivity properties of molecular systems can also be assessed by calculations of Fukui functions, quantum molecular descriptors that indicate how the electron density changes with the addition or removal of a charge. In this work, the Fukui functions were calculated by the Jaguar program within the framework of the finite difference approach, according to the following equations:

$$f^+ = \frac{\left(\rho^{N+\delta}(r) - \rho^N(r)\right)}{\delta} \quad (2)$$

$$f^- = \frac{\left(\rho^{N-\delta}(r) - \rho^N(r)\right)}{\delta} \quad (3)$$

* 1 bohr = 5.29×10^{-11} m

where N stands for the number of electrons in the reference state of the molecule, while δ stands for the fraction of an electron the default value of which is set to be 0.01.[67]

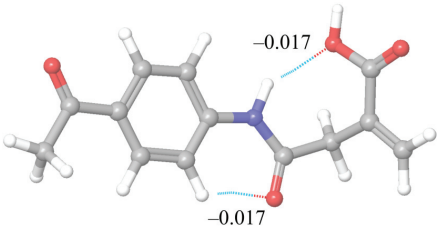

Fig. 6. Intramolecular non-covalent interactions and their strengths (in electron/bohr^3) of 4-[(4--acetylphenyl)amino]-2-methylidene-4-oxobutanoic acid.

Visualization of the Fukui functions was performed by mapping the f^+ and f^- values to the electron density surface as well (Fig. 7). The purple colour was used as the positive colour in the case of visualization of Fukui f^+ (Fig. 7a) and it emphasizes molecule sites with increased electron density after addition of charge. The red colour was used as the positive colour in the case of the visualization of the Fukui f^- function (Fig. 7b) and it emphasizes molecule sites with decreased electron density after charge was removed. According to the results presented in Fig. 7a, it could be concluded that after charge addition, the electron density increases in the near vicinity of carbon atom C14, indicating that this molecule site acts as an electrophile upon charge addition. On the other hand, according to the results presented in Fig. 7b, it could be concluded that after charge removal, the electron density decreases in the oxygen atom O3 and carbon atom C9, designating these molecule sites as nucleophilic upon charge removal.

Nonlinear optical properties

A nonlinear optical (NLO) effect arises from the interactions of electromagnetic fields in various media to produce new fields altered in phase, frequency, amplitude or other propagation characteristics from the incident fields.[68] NLO properties such as the dipole moment, polarizability, first and second order hyperpolarizabilites are calculated using B3LYP/6-311++G(d) (5D, 7F). The total molecular dipole moment of the title compound is 3.408 D*, the polarizability is 2.714×10^{-23} esu**, and the first and second order hyperpolarizabilities are 6.268×10^{-30} and -15.928×10^{-37} esu. Here, the first hyperpolarizability of the title compound is 48.22 times that of the standard NLO material urea,[69] and comparable with the reported values of similar derivatives.[45,70] The larger component of the second order hyperpolarizability is associated with the larger ground state polarization that leads to strong electronic coupling between the ground and the low lying excited state. The NLO properties are also related to the energy gap

* 1 D = 3.34×10^{-30} C m
** 1 a.u. = 8.6393×10^{-33} esu

between the HOMO and LUMO. The energy gap of the investigated compound is 4.332 eV, which is lower than that of urea (6.7 eV).[69] Therefore, the investigated molecule is considered a good candidate for nonlinear optical applications.

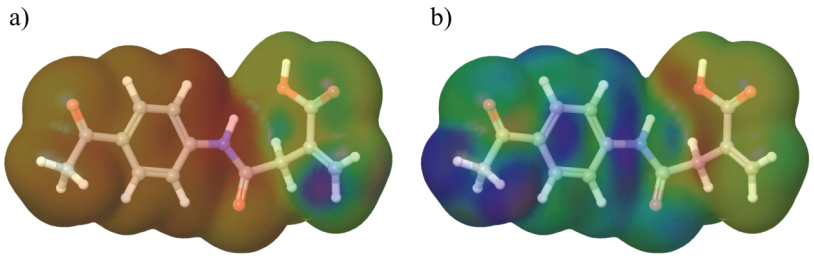

Fig. 7. Fukui functions: a) f^+ and b) f^- of 4-[(4-acetylphenyl)amino]-2-methylidene-4-oxobutanoic acid.

Natural bond orbital analysis

The calculations of the natural bond orbitals (NBO) were performed using the NBO 3.1 program[71] as implemented in the Gaussian09 package at the DFT/B3LYP level in order to understand various second-order interactions as given in Tables S-3 and S-4 of the Supplementary material. The orbital overlap between n(O) and n(N) and σ*(C–O), π*(C–O), σ*(C–C) and σ*(C–N) bond orbitals give strong intermolecular hyperconjugative interactions with stabilization energies of 26.63, 36.97, 40.87, 20.48 and 60.78 KJ mol^{-1}, and the interactions are: N_6–C_8 from O_1 of $n_2(O_1)\rightarrow\sigma^*(N_6–C_8)$, C_{13}–O_3 from O_2 of $n_2(O_2)\rightarrow$ $\rightarrow\sigma^*(C_{13}–O_3)$, C_{13}–O_2 from O_3 of $n_2(O_3)\rightarrow\pi^*(C_{13}–O_2)$, C_{27}–C_{28} from O_5 of $n_2(O_5)\rightarrow\sigma^*(C_{27}–C_{28})$, C_8–O_1 from N_6 of $n_1(N_6)\rightarrow\pi^*(C_8–O_1)$ with electron densities of 0.07744, 0.11051, 0.23906, 0.05316 and 0.26733 e, respectively. The higher energy orbitals with p-character around 100 % are, $n_2(O_1)$, $n_2(O_2)$, $n_2(O_3)$ and $n_2(O_5)$ having energies of –0.25478, –0.27969, –0.36214, –0.24789 a.u, respectively, and possess low occupation numbers of 1.85987, 1.83353, 1.83540 and 1.89069, respectively. The lower energy orbitals are: $n_1(O_1)$, $n_1(O_2)$, $n_1(O_3)$ and $n_1(O_5)$ with energies of –0.68016, –0.70320, –0.64024 and –0.66999 a.u., and these orbitals possess high occupation numbers of 1.97381, 1.97594, 1.96940 and 1.97772, respectively, with p-characters of 42.26, 42.20, 55.92 and 43.20 %, respectively.

Reactive and degradation properties based on autoxidation and hydrolysis

Determination of degradation mechanism is very important for the development of procedures for the removal of organic pollutants from aquatic media. However, this is not an easy task, but it could be rationalized and optimized by employment of DFT calculations and MD simulations. In particular, the possibility of an autoxidation mechanism, very important for the determination or

confirmation of the degradation path of some organic pharmaceutical molecules could be assessed by calculations of the *BDE* for hydrogen abstraction.[62–75] A molecule is considered suitable for an autoxidation mechanism when the *BDE* values are in the appropriate range. If the *BDE* values fall in the range between 75 to 85 kcal mol^{-1},[76,77] the molecule could be considered as very sensitive to an autoxidation mechanism. Values between 70 to 75 kcal mol^{-1} and between 85 and 90 kcal mol^{-1} could also be taken into consideration.[78] On the other hand, values lower than 70 kcal mol^{-1} are not suitable for the autoxidation mechanism.[22,76,78] At the same time, *BDE* values for the rest single acyclic bonds might serve as indicators of molecule sites where degradation could commence. All *BDE* values for the investigated molecule are shown in Fig. S-3 of the Supplementary material.

From the aspect of autoxidation mechanism there is one site of investigated molecule which could be interesting. The bond denoted number 3 has a *BDE* value for hydrogen abstraction of ≈87 kcal mol^{-1} is considered low enough for the start of an autoxidation mechanism. Simultaneously, all other BDE values for hydrogen abstraction are too high to be considered as interesting for an autoxidation mechanism. The lowest *BDE* value for the other single acyclic bonds was calculated for the bond denoted with number 10, with value of ≈69 kcal mol^{-1}. The aforementioned BDE values are similar, actually they are adjacent and hence, it can be stated that degradation of title molecule could start precisely at these locations.

The atoms of the investigated molecule have very pronounced interactions with water molecules according to the radial distribution functions (RDFs) shown in Fig. 8. The RDF, $g(r)$, indicates the probability of finding a particle at a distance r from another particle.[79] According to the obtained results shown in Fig. S-3, both carbon (Fig. 8a) and non-carbon (Fig. 8b) atoms have significant interactions with water molecules. The carbon atoms C8, C14 and C28 have very similar values of the peak distance at around 3.5 Å, with the carbon atom C28 having the highest maximal $g(r)$ value of around 1.3. The highest maximal $g(r)$ value, around 1.5, was calculated for carbon atom C12 while its peak distance is located at around 4.7 Å. As expected, much more significant interactions with water molecules were determined for oxygen atoms O1and O3 and for hydrogen atoms H4 and H7.

Both oxygen atoms have practically the same value of the peak distance located at around 2.6 Å, with oxygen atom O1 having a much sharper $g(r)$ profile, indicating much more pronounced interactions with water molecules. Peak distance of O7 is located at around 1.8 Å, while its maximal $g(r)$ value is between 0.8 and 0.9. The strongest interactions with water molecules were determined for hydrogen atoms H4 and H7. The strongest interaction with water molecules was certainly determined for hydrogen atom H4, the peak distance of which is located at around 1.6 Å, while its maximal $g(r)$ value, almost 1.8, is the highest of all the values calculated in this

work. The very interesting RDF values in the case of the title molecule indicate that the hydrolysis mechanism could play a significant role in the degradation.

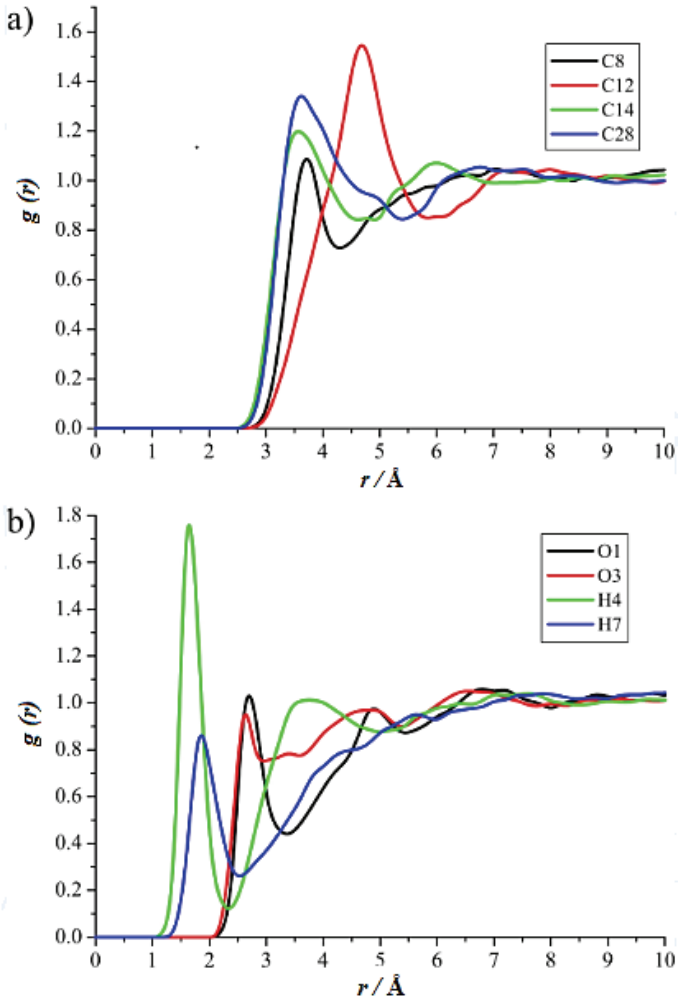

Fig. 8. RDF values of: a) the C atoms and b) the O and H atoms of the 4-[(4-acetylphenyl)-amino]-2-methylidene-4-oxobutanoic acid molecule with significant interactions with water molecules.

Molecular docking studies

The insulin receptor kinase (IRK) is a $\alpha_2\beta_2$ heterotetrameric glycoprotein possessing intrinsic protein tyrosine kinase (PTK) activity.[80] Upon insulin binding to the α subunits, the insulin receptor undergoes a poorly characterized conformational change that results in autophosphorylation of specific tyrosine resi-

dues in the cytoplasmic portion of the β subunits.[81,82] The high resolution crystal structure of the protein target was downloaded from the protein data bank website (PDB ID: 1I44).[83] All molecular docking calculations were performed on AutoDock Vina software.[84,85] The docking protocol predicted the same conformation as was present in the crystal structure with an *RMSD* value well within the reliable range of 2 Å.[86] Amongst the docked conformations, one which binds well at the active site was analysed for detailed interactions in Discover Studio Visualizer 4.0 software and the ligand binds at the active site of the substrate (Fig. 9 and Fig. S-4 of the Supplementary material) by conventional hydrogen bonds and pi–amide stacking interactions. The amino acids Ser1090 and Leu1002 form H-bonds with the OH group and carbonyl oxygen. His1081 forms a pi–amide stacking interaction with the benzene ring. The docked ligand title compound forms a stable complex with CDK4 and gives a binding affinity (ΔG in kcal mol^{-1}) value of –10.2 (Table S-V of the Supplementary material).

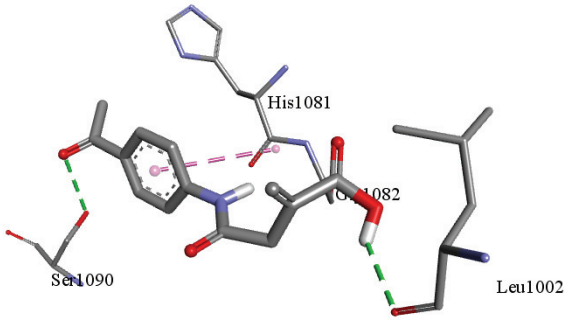

Fig. 9. Detailed interaction of amino acids of the receptor with the ligand.

CONCLUSIONS

Using the B3LYP/6-311++G(d) (5D, 7F) basis set, the structure, vibrational wave numbers, molecular electrostatic potential and nonlinear optical properties of the title compound were determined, and natural bond orbital analysis was realised. The most reactive sites for electrophilic and nucleophilic attacks were identified using MEP analysis. The calculated first hyperpolarizability is 48.22 times that of the standard NLO material urea. Visualization of the *ALIE* values by their mapping to the electron density surface indicate three molecule sites possibly prone to electrophilic attacks – the benzene ring, the near vicinity of the oxygen atom O5 and the near vicinity of carbon atom C9. The highest *ALIE* value was determined at hydrogen atom H4, which also has the most pronounced interactions with water molecules according to the RDF values. According to the Fukui functions, the carbon atoms C9, C14 and oxygen atom O3 were also proved as possible important reactive centres. The *BDE* for hydrogen abstraction indicated that the autoxidation mechanism could be possible at the location of the hydrogen atom H10, as *BDE* value for hydrogen abstraction in this case is ≈87

kcal mol^{-1}. The calculated RDF values indicated several atoms with pronounced interactions with water molecules and that hydrolysis could have a significant influence in the degradation of the title molecule. From the molecular docking studies, the amino acids Ser1090 and Leu1002 of CDK4 form H-bonds with OH group and carbonyl oxygen and His1081 forms pi–amide stacking interaction with the benzene ring.

SUPPLEMENTARY MATERIAL

Supplementary material pertaining to the title compound is available electronically from http://www.shd.org.rs/JSCS/, or from the corresponding author on request.

Acknowledgement, The authors would like to extend their sincere appreciation to the Deanship of Scientific Research at King Saud University for funding this work through the Research Group Project No. RG-1435-062. The support received from Schrödinger Inc. is greatly appreciated.

ИЗВОД

4-[(4-АЦЕТИЛФЕНИЛ)АМИНО]-2-МЕТИЛИДЕН-4-ОКСОБУТАНСКА КИСЕЛИНА, НОВОСИНТЕТИСАНИ АМИД СА ХИДРОФИЛНИМ И ХИДРОФОБНИМ ЕЛЕМЕНТИМА: СПЕКТРОСКОПСКА КАРАКТЕРИЗАЦИЈА И ИЗУЧАВАЊЕ РЕАКТИВНИХ ОСОБИНА

SHEENA Y. MARY[1], EBTEHAL S. AL-ABDULLAH[2], HAYA I. ALJOHAR[2], BADIADKA NARAYANA[3], PRAKASH S. NAYAK[3], BALADKA K. SAROJINI[4], STEVAN ARMAKOVIĆ[5], SANJA J. ARMAKOVIĆ[6], CHRISTIAN VAN ALSENOY[7] и ALI A. EL-EMAM[2]

[1]Department of Physics, Fatima Mata National College, Kollam, Kerala, India, [2]Department of Pharmaceutical Chemistry, College of Pharmacy, King Saud University, Riyadh 11451, Saudi Arabia, [3]Department of Studies in Chemistry, Mangalore University, Mangalagangothri, Mangalore 574199, India, [4]Department of Studies in Industrial Chemistry, Mangalore University, Mangalagangothri, Mangalore 574199, India, [5]Универзитет у Новом Саду, Природно–математички факултет, Одсек за физику, Трг Д. Обрадовића 4, 21000 Нови Сад, [6]Универзитет у Новом Саду, Природно–математички факултет,Одсек за хемију, биохемију и заштиту околине, Трг Д. Обрадовића 3, 21000 Нови Сад и [7] Department of Chemistry, University of Antwerp, Groenenborgerlaan 171, B-2020, Antwerp, Belgium

Снимљени су FT-IR и FT-раманski спектри 4-[(4-ацетилфенил)амино]-2-метилиден-4-оксобутанске киселине. Вибрациони таласни бројеви су израчунати DFT квантнохемијским израчунавањима и приписивање вибрација је урађено користећи расподелу потенцијалне енергије. Теоријски предвиђени геометријски параметри су у сагласности са XRD подацима. Одређивање и визуелизација места у молекулу која су погодна за електрофилни напад је урађено мапирањем просечних локалних енергија јонизације (*ALIE*) на површину електронске густине. Даље одређивање могућих реактивних центара проучаваног молекула је урађено израчунавањем Fukui функције. Интрамолекулске нековалентне интеракције су такође биле одређене и визуелизоване. Предвиђање места у молекулу погодних за аутооксидацију је такође урађено израчунавањем енергија дисоцијације везе (*BDE*), док је стабилност проучаваног молекула у води процењена израчунавањем функције радијалне расподеле (RDF) добијене након симулације молекулском динамиком (MD). Проучавано једињење доковано као лиганд формира стабилан комплекс са CDK4 и даје афинитет везивања од –10,2 kcal mol^{-1}.

(Примљено 3. јануара 2017, ревидирано 17. марта, прихваћено 16. маја 2017)

REFERENCES

1. M. B. Milovanović, S. Trifunović, L. Katsikas, I. G. Popović, *J. Serb. Chem. Soc.* **72** (2007) 1507

2. M. A. R. Meirer, J. O. Metzger, U. S. Schubert, *Chem. Soc. Rev.* **36** (2007) 1788
3. N. P. Shetgiri, B. K. Nayak, *Indian J. Chem., B* **44** (2005) 1933
4. S. Katla, P. Pothana, B. Gubba, S. Manda, *Der Chem. Sin.* **2** (2011) 47
5. H. D. Hanoon, *Iraqi Natt. J. Chem.* **41** (2011) 77
6. P. S. Nayak, B. Narayana, J. P. Jasinski, H. S. Yathirajan, M. Kaur, *Acta Crystallogr. E* **69** (2013) o1752
7. D. Galankis, A. P. Kourounakis, K. C. Tsiakitzis, C. Doulgkeris, E. A. Rekka, A. Gavalas, C. Kravaritou, C. Christos, P. N. Kourounakis, *Bioorg. Med. Chem. Lett.* **14** (2004) 3639
8. P. Kumar, E. E. Knaus, *Eur. J. Med. Chem.* **28** (1993) 881
9. M. Ban, H. Taguchi, T. Katushima, M. Takahashi, K. Shinoda, A. Watanabe, T. Tominaga, *Bioorg. Med. Chem.* **6** (1998) 1069
10. I. V. Ukrainets, L. V. Sidorenko, L. A. Petrushovo, O. V. Gorokhova, *Chem. Heterocycl. Compd.*(N.Y., NY, U.S.) **42** (2006) 64
11. R. B. Lesyk, B. S. Zimenkovsky, *Curr. Org. Chem.* **8** (2004) 1547
12. V. Gududru, E. Hurh, J. T. Dalton, D. D. Miller, *Bioorg. Med. Chem. Lett.* **14** (2004) 5289
13. S. Armaković, S. J. Armaković, J. P. Šetrajčić, I. J. Šetrajčić, *J. Mol. Model.* **18** (2012) 4491
14. B. Abramović, S. Kler, D. Šojić, M. Laušević, T. Radović, D. Vione, *J. Hazard. Mater.* **198** (2011) 123
15. S. J. Armaković, S. Armaković, N. L. Finčur, F. Šibul, D. Vione, J. P. Šetrajčić, B. Abramović, *RSC Adv.* **5** (2015) 54589
16. M. Blessy, R. D. Patel, P. N. Prajapati, Y. Agrawal, *J. Pharm. Anal.* **4** (2014) 159
17. J. Molnar, J. Agbaba, B. Dalmacija, M. Klašnja, M. Watson, M. Kragulj, *J. Environ. Eng.* **138** (2011) 804
18. J. J. Molnar, J. R. Agbaba, B. D. Dalmacija, M. T. Klašnja, M. B. Dalmacija, M. M. Kragulj, *Sci. Total Environ.* **425** (2012) 169
19. D. V. Šojić, D. Z. Orčić, D. D. Četojević-Simin, N. D. Banić, B. F. Abramović, *Chemosphere* **138** (2015) 988
20. D. V. Šojić, D. Z. Orčić, D. Četojević-Simin, *J. Mol. Catal., A: Chem.* **392** (2014) 67
21. D. D. Četojević-Simin, S. J. Armaković, D. V. Šojić, B. F. Abramović, *Sci. Total Environ.* **463** (2013) 968
22. P. Lienard, J. Gavartin, G. Boccardi, M. Meunier, *Pharm. Res.* **32** (2015) 300
23. G. L. de Souza, L. M. de Oliveira, R. G. Vicari, A. Brown, *J. Mol. Model.* **22** (2016) 100
24. Z. Sroka, B. Żbikowska, J. Hładyszowski, *J. Mol. Model.* **21** (2015) 307
25. H. Djeradi, A. Rahmouni, A. Cheriti, *J. Mol. Model.* **20** (2014) 2476
26. B. Narayana, P. S. Nayak, B. K. Sarojini, J. P. Jasinski, *Acta Crystallogr. E* **70** (2014) o752
27. *Gaussian-09, Revision B.01*, Gaussian Inc., Wallingford CT, 2009
28. J. B. Foresman, A. Frisch, *Exploring Chemistry with Electronic Structure Methods*, Gaussian Inc., Pittsburgh, PA, 1996
29. R. Dennington, T. Keith, J. Millam, *Gaussview*, *Version 5*, Semichem Inc., Shawnee-Mission KS, 2009
30. J. M. L. Martin, C. Van Alsenoy, *GAR2PED*, *A Program to Obtain a Potential Energy Distribution from a Gaussian Archive Record*, University of Antwerp, 2007
31. A. D. Bochevarov, E. Harder, T. F. Hughes, J. R. Greenwood, D. A. Braden, D. M. Philipp, D. Rinaldo, M. D. Halls, J. Zhang, R. A. Friesner, *Int. J. Quantum Chem.* **113** (2013) 2110

32. D. Shivakumar, J. Williams, Y. Wu, W. Damm, J. Shelley, W. Sherman, *J. Chem. Theory Comput.* **6** (2010) 1509
33. Z. Guo, U. Mohanty, J. Noehre, T. K. Sawyer, W. Sherman, G. Krilov, *Chem. Biol. Drug Des.* **75** (2010) 348
34. I. Fabijanić, C. J. Brala, V. Pilepić, *J. Mol. Model.* **21** (2015) 99
35. A. D. Becke, *J. Chem. Phys.* **98** (1993) 5648
36. J. L. Banks, H. S. Beard, Y. Cao, A. E. Cho, W. Damm, R. Farid, A. K. Felts, T. A. Halgren, D. T. Mainz, J. R. Maple, *J. Comput. Chem.* **26** (2005) 1752
37. H. J. Berendsen, J. P. Postma, W. F. van Gunsteren, J. Hermans, *Interaction models for water in relation to protein hydration,* in *Intermolecular forces*, Springer, Berlin, 1981, pp. 331–342
38. A. Otero-de-la-Roza, E. R. Johnson, J. Contreras-García, *Phys. Chem. Chem. Phys.* **14** (2012) 12165
39. E. R. Johnson, S. Keinan, P. Mori-Sanchez, J. Contreras-García, A. J. Cohen, W. Yang, *J. Am. Chem. Soc.* **132** (2010) 6498
40. *Schrödinger Release 2015-4, Maestro, version 10.4*, Schrödinger, LLC, New York, 2015
41. T. Lu, F. Chen, *J. Comput. Chem.* **33** (2012) 580
42. T. Lu, F. Chen, *J. Mol. Graphics Modell* **38** (2012) 314
43. L. Tian, C. Feiwu, *Acta Chim. Sin.* **69** (2011) 2393
44. M. Xiao, T. Lu, *J. Adv. Phys. Chem.* **4** (2015) 111
45. R. Raju, C. Y. Panicker, P. S. Nayak, B. Narayana, B. K. Sarojini, C. Van Alsenoy, A. A. Al-Saadi, *Spectrochim. Acta, A* **134** (2015) 63
46. T. Rajamani, S. Muthu, *Solid State Sci.* **16** (2013) 90
47. R. Minitha, Y. S. Mary, H. T. Varghese, C. Y. Panicker, R. Ravindran, K. Raju, V. M. Nair, *J. Mol. Struct.* **985** (2011) 316
48. Y. S. Mary, K. Raju, I. Yildiz, O. T. Arpaci, H. I. S. Nogueira, C. M. Grandadeiro, C. Van Alsenoy, *Spectrochim. Acta, A* **96** (2012) 617
49. N. P. G. Roeges, *A Guide to the Complete Interpretation of IR Spectra of Organic Compounds*, Wiley, New York, 1994
50. N. B. Colthup, L. H. Daly, S. E. Wiberly, *Introduction of Infrared and Raman Spectroscopy*, Academic Press, New York, 1975
51. G. Socrates, *Infrared Characteristic Group Frequencies*, Wiley, New York, 1981
52. L. J. Bellamy, *The Infrared Spectrum of Complex Molecules*, 3rd ed., Chapman and Hall, London, 1975
53. Y. S. Mary, H. T. Varghese, C. Y. Panicker, M. Dolezal, *Spectrochim. Acta, A* **71** (2008) 725
54. R. M. Silverstein, G. C. Bassler, T. C. Morril, *Spectrometric Identification of Organic Compounds*, 5th ed., Wiley, Singapore, 1991
55. G. Varsanyi, *Assignments of Vibrational Spectra of Seven Hundred Benzene Derivatives*, Wiley, New York, 1974
56. K. Fukui, T. Yonezawa, H. Shingu, *J. Chem. Phys.* **20** (1952) 722
57. S. Gunasekaran, R. A. Balaji, S. Kumaresan, G. Anand, S. Srinivasan, *Can. J. Anal. Sci. Spectrosc.* **53** (2008) 149
58. R. J. Parr, R. G. Pearson, *J. Am. Chem. Soc.* **105** (1983) 7512
59. I. Ajaj, J. Markovski, J. Marković, M. Jovanović, M. Milčić, F. Assaleh, A. Marinković, *Struct. Chem.* **25** (2014) 1257
60. T. Le Bahers, C. Adamo, I. Ciofini, *J. Chem. Theor. Comput.* **7** (2011) 2498

61. C. A. Guido, P. Cortona, B. Mennucci, C. Adamo, *J. Chem. Theory Comput*. **9** (2013) 3118
62. G. Keresztury, S. Holly, G. Besenyei, J. Varga, A. W. Wang, J. R. Durig, *Spectrochim. Acta, A* **49** (1993) 2007
63. J. S. Murray, J. M. Seminario, P. Politzer, P. Sjoberg, *Int. J. Quantum Chem.* **38** (S24) (1990) 645
64. P. Politzer, F. Abu-Awwad, J. S. Murray, *Int. J. Quantum Chem.* **69** (1998) 607
65. F. A. Bulat, A. Toro-Labbé, T. Brinck, J. S. Murray, P. Politzer, *J. Mol. Model.* **16** (2010) 1679
66. P. Politzer, J. S. Murray, F. A. Bulat, *J. Mol. Model.* **16** (2010) 1731
67. A. Michalak, F. De Proft, P. Geerlings, R. Nalewajski, *J. Phys. Chem., A* **103** (1999) 762
68. Y. X. Sun, Q. L. Hao, W. X. Wei, Z. X. Yu, L. D. Lu, X. Wang, Y. S. Wang, *J. Mol. Struct.: THEOCHEM* **904** (2009) 74
69. C. Adant, M. Dupuis, J. L. Bredas, *Int. J. Quantum Chem.* **56** (1995) 497
70. Y. S. Mary, C. Y. Panicker, H. T. Varghese, K. Raju, T. E. Bolelli, I. Yildiz, C. M. Granadeiro, H. I. S. Nogueira, *J. Mol. Struct.* **994** (2011) 223
71. E. D. Glendening, A. E. Reed, J. E. Carpenter, F. Weinhold, *NBO 3.1 Program Manual,* Theoretical Chemistry Institute, University of Wisconsin, Madison, WI
72. X. Ren, Y. Sun, X. Fu, L. Zhu, Z. Cui, *J. Mol. Model.* **19** (2013) 2249
73. L. L. Ai, J. Y. Liu, *J. Mol. Model.* **20** (2014) 2179
74. W. Sang-Aroon, V. Amornkitbamrung, V. Ruangpornvisuti, *J. Mol. Model.* **19** (2013) 5501
75. J. Kieffer, É. Brémond, P. Lienard, G. Boccardi, *J. Mol. Struct.: THEOCHEM* **954** (2010) 75
76. J. S. Wright, H. Shadnia, L. L. Chepelev, *J. Comput. Chem.* **30** (2009) 1016
77. G. Gryn'ova, J. L. Hodgson, M. L. Coote, *Org. Biomol. Chem.* **9** (2011) 480
78. T. Andersson, A. Broo, E. Evertsson, *J. Pharm. Sci.* **103** (2014) 1949
79. R. V. Vaz, J. R. B. Gomes, C. M. Silva, *J. Supercrit. Fluids* **107** (2016) 630
80. A. Ullrich, J. R. Bell, E. Y. Chen, R. Herrera, L. M. Petruzzelli, T. J. Dull, A. Gray, L. Coussens, Y. C. Liao, M. Tsubokawa, P. H. Seeburg, C. Grunfeld, O. M. Rosen, J. Ramachandran, *Nature* **313** (1985) 756
81. H. E. Tornqvist, M. W. Pierce, A. R. Frackelton, R. A. Nemenoff, J. Avruch, *J. Biol. Chem.* **262** (1987) 10212
82. J. M. Tavare, R. M. O'Brien, K. Siddle, R. M. Denton, *Biochem. J.* **253** (1988) 783
83. J. H. Till, A. J. Ablooglu, M. Frankel, S. M. Bishop, R. A. Kohanski, S. R. Hubbard, *J. Biol. Chem.* **276** (2001) 10049
84. O. Trott, A. J. Olson, *J. Comput. Chem.* **31** (2010) 455
85. R. I. Al-Wabli, K. S. Resmi, Y. S. Mary, C. Y. Panicker, M. I. Attia, A. A. El-Emam, C. Van Alsenoy, *J. Mol. Struct.* **1123** (2016) 375
86. B. Kramer, M. Rarey, T. Lengauer, *Proteins* **37** (1999) 228.